Analysis of the Operation of an Integrated Unidirectional Phase Modulator

T. T. M. van Schaijk, D. Lenstra, K. A. Williams and E. A. J. M. Bente
Eindhoven University of Technology, Den Dolech 2, 5612AZ Eindhoven, The Netherlands
Tel: +31402473728, Email: p.v.schaijk@tue.nl

ABSTRACT

In this paper we present a model and experimental verification of a unidirectional phase modulator realised in InP. We show that non-linearity in the phase-voltage dependance of the electro-refractive modulators has to be taken into account. It limits the isolation that can be obtained using the device and it introduces modulation on the forward propagating wave. Finally we derive minimum requirements for the electrical driving signals that allow operation of the unidirectional phase modulator close to this optimal performance such that its performance is limited by non-linearity only. In this way, we find for our device a maximum tolerable imbalance in modulation amplitude of $2\,\%$, a phase error of $0.18°$ and an error in the summed modulation amplitude of the two driving signals of $2.8\,\%$. These values are feasible with current electronics.

Keywords: integrated isolator, optical isolator, unidirectional phase modulator, photonic integration

1 INTRODUCTION

Many optical circuits require a strong optical isolator to prevent the deleterious effects on the performance of the system that are caused by light that is reflected back into the circuit. Most notably optical isolators are used to protect lasers from external optical feedback (EOF), requiring as much as $60\,\mathrm{dB}$ isolation. Deployed photonic circuits require isolation against reflections and optical disturbances from outside the chip. It has proven difficult to achieve strong isolation in a monolithically integrated platform using magneto-optic effects [1], mainly because the required magnetically active materials strongly attenuate the light and are often incompatible with clean room processes used for fabricating photonic integrated circuits (PICs).

A different approach to realizing an integrated isolator using directionally dependent properties of tandem sinusoidally driven phase modulators is presented in [2]. The tandem phase modulators we shall refer to as a unidirectional phase modulator (UPM) and are schematically depicted in Fig. 1. Combining the UPM with a spectral filter yields a significant difference in directionally dependent loss for light of a single optical frequency, e.g. as from a single mode laser. Using this approach, [2] demonstrated $10.8\,\mathrm{dB}$ of isolation. This is insufficient to protect lasers from strong EOF when the isolator is placed in series with the laser. However, we have predicted that this amount of isolation can be used within an integrated, unidirectional ring laser to create greatly enhanced reflection tolerance [3]. In such a laser, the performance of the UPM, when integrated into the laser cavity, has a big impact on quality of the emitted laser light. It is therefore important to characterize the performance of the UPM in detail and derive its optimal parameters for operation.

2 UPM MODEL AND VERIFICATION

We start our model with the description of individual InP-based ridge wave guide phase modulators. Then the model is extended to two modulators. Each phase modulator is implemented using a voltage controlled electro-refractive modulator (ERM) and is modeled as a time-dependent, non-linear, local variation of the refractive index that is a function of the applied voltage. Non-linear effects are taken into account up to second order.

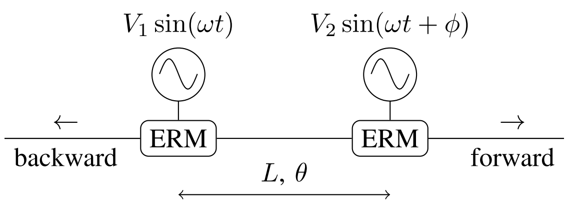

Figure 1. Schematic representation of a UPM consisting of two tandem ERMs. Both modulators are driven by an RF signal with potentially different amplitude and at a phase difference ϕ. The modulators are spaced by a distance L. Due to the finite group velocity, the electrical signal has gained $\theta \equiv \omega L/v_g$ phase while the light is traveling this distance.

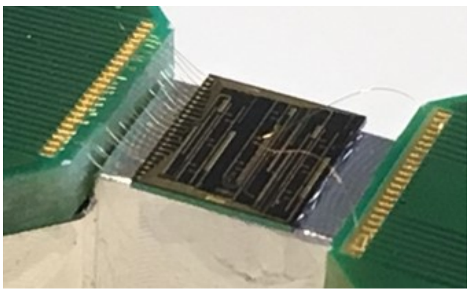

Figure 2. Photograph of the fabricated PIC which contains a number of devices among which the UPM presented here. The structure connected to the PCB on the right is the UPM described in this paper.

Residual amplitude modulation (RAM) is assumed to scale linearly with refractive index modulation. On the fabricated PIC both modulators are positioned $300\,\mu\mathrm{m}$ apart, so their characteristics are assumed to be identical.

The electrical signals driving the ERMs are assumed to have the same frequency. In practice this assumption can be satisfied relatively easily if both electrical signals are derived from the same source or from two phase locked sources. As can be seen in Fig. 1, there is a phase difference ϕ between the driving signals and there is a length L of waveguide separating the two ERMs. It takes the light a finite amount of time to travel between these two modulators and therefore the time at which the light is modulated is different for each modulator. We assume the waveguide separating the ERMs has no effect on the light other than the time delay. This allows us to model both ERMs as if they are located at the same physical location by introducing an additional effective phase delay $\theta \equiv \pm\omega L/v_g$ which is positive for light propagating in the forward direction and negative for light propagating in the backward direction. We model the complete UPM as the sum of two ERMs driven by sinusoidal voltages with phase difference $\psi \equiv \phi + \theta$, which is dependent on the propagation direction of the light. This direction dependence is the effect that is used to ultimately obtain isolation using the UPM and it is therefore crucial to its operation.

From the effective modulation of the refractive index follows the phase modulation amplitude $2\pi L n(t)/\lambda$ where $n(t)$ is the change in refractive index at time t and λ is the wavelength of the light. The phase modulation amplitudes imposed by both modulators are called A_1 and A_2 respectively. From this we define the average modulation amplitude $A \equiv (A_1 + A_2)/2$, the modulation imbalance $\alpha \equiv (A_1 - A_2)/(A_1 + A_2)$, the proportionality constant for RAM γ and the proportionality constant for non-linearity β. It can be shown that the modulated spectrum is a frequency comb with peaks spaced at the electrical frequency ω. The intensity of the comb lines depend on the properties of the UPM and its driving signals and is found as

$$P_k \equiv P\left|\sum_{m=-\infty}^{\infty} i^m J_{k-2m}(B_1) J_m(B_2) \exp\big((k-2m)\Psi_1 + m\Psi_2\big)\right|^2 \tag{1}$$

where

$$B_1 \equiv A(1-j\gamma)\sqrt{2+2\alpha^2+2(1-\alpha^2)\cos\psi}, \tag{2}$$

$$B_2 \equiv -\frac{1}{2}A(1-j\gamma)\beta\sqrt{2+2\alpha^2+2(1-\alpha^2)\cos(2\psi)}, \tag{3}$$

$$\tan\Psi_m \equiv \frac{(1-\alpha)\sin m\psi}{(1+\alpha)+(1-\alpha)\cos m\psi} \tag{4}$$

represent the effective first and second order modulation amplitudes and the effective modulation phase respectively, P is the input power and k denotes the order of the side band as counted from the center.

3 EXPERIMENTAL VERIFICATION

Our model was verified using a UPM that was manufactured in the SMART photonics InP based platform [4] and that is shown in Fig. 2. The ERMs were deeply etched, had a length of $1\,\mathrm{mm}$ and were separated by deeply-etched waveguide such that the spacing of their centers was $L = 4167\,\mu\mathrm{m}$. This optimizes operation for $5\,\mathrm{GHz}$. In the experiments, the ERMs were connected to two signal generators via bond wires, a PCB and coaxial cables. Two signal generators were phase-locked to each other with a controllable RF phase difference ϕ. The electrical modulation frequency ω corresponded to $3.5\,\mathrm{GHz}$ because of limitations in the transmission of the electrical connections. The output from a tunable laser (HP 81940A) set at $1550\,\mathrm{nm}$ and $10\,\mathrm{mW}$ was coupled into the PIC via a lensed fibre and was sent through the UPM. The comb generated by the UPM was measured using an optical spectrum analyser with $20\,\mathrm{MHz}$ resolution (APEX 2641-B).

In the experiments the ERMs were biased at $-6\,\mathrm{V}$. One of the signal generators was set at a modulation amplitude of $3.2\,\mathrm{Vp}$, while the other was swept from $2.1\,\mathrm{Vp}$ to $3.2\,\mathrm{Vp}$ in steps of $0.16\,\mathrm{Vp}$. Subsequently the second modulator was kept at $3.2\,\mathrm{Vp}$ while the other was swept in amplitude. For each set of modulation amplitudes the phase difference between the signal generators was swept over $360°$ in steps of $10°$. Finally, the whole procedure was performed four additional times to determine the non-systematic errors. Fig. 3 shows the mean and standard deviation of the measured values as error bars for two settings of the modulation amplitude. The solid line in this figure shows the result of a fit of the modeling parameters to all experimental data simultaneously. Very good agreement is obtained, validating the model.

4 REQUIREMENTS ON ELECTRICAL DRIVING SIGNALS

The model allows one to study the effects of the electrical signals driving the ERMs on the performance of the UPM. Non-linearity in the phase response of the ERMs mainly influences the suppression of the central band of a backward propagating wave, as well as the power in the even side bands for a forward propagating wave. It can be neglected for other properties of the UPM.

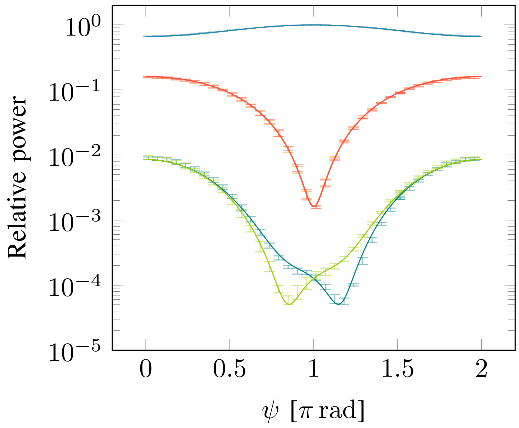

Figure 3. Relative intensity of the sidebands as measured at the output of the UPM as a function of the effective phase difference for $\alpha = -0.09$ (left) and $\alpha = 0.005$ (right). The sidebands are centered at the optical input frequency and spaced by the electrical driving frequency. Sidebands -2, ..., 2 are presented in green, orange, blue, red and cyan respectively. The error bars indicate the mean and standard deviation of the experimental data, the solid line is the fitted data. Our model captures the characteristics of the UPM very well as can be seen from the good fit.

From our experiment, we find that non-linearity limits isolation to approximately $26\,\mathrm{dB}$, taking all other values optimal. Allowing other effects to reduce this number by $1\,\mathrm{dB}$ we find a maximum tolerable imbalance in the modulation amplitudes of both ERMs of $\alpha = 0.02$, a maximum error in the phase difference of $\psi = 0.18°$ and a maximum error in the modulation amplitude of $A = 2.5\,\%$ or $1.46°$ at the optimum modulation amplitude.

For the forward direction Fig. 3 shows that non-linearity in the ERMs causes second order side bands at approximately $-40\,\mathrm{dB}$. For optimal isolation the ERMs need to be driven at a higher voltage, increasing these sidebands to approximately $-24\,\mathrm{dB}$. We take this value as the maximum allowable power for the first order side bands. From (1) and using $B_2 = 0$, we find a requirement on the modulation amplitude for light propagating in the forward direction, which is satisfied if $A\sqrt{2 + 2\alpha^2 + 2(1 - \alpha^2)\cos\psi} < 0.13\,\mathrm{rad}$. From this we find the maximum tolerable modulation imbalance $\alpha < 0.054$ and the maximum tolerable error in the electrical phase difference ψ of $6.2°$. Any error in A does not affect the first order side bands up to a first order approximation.

5 CONCLUSION

A UPM was fabricated and characterized and a phenomenological model was derived to describe the performance of the UPM. Very good agreement was found between the experimental data and the model. It was shown that non-linearity in the phase transfer function of the ERMs limits the isolation that can be achieved using such a UPM as well as the maximum suppression of side bands generated in the forward propagating light. We derived minimum requirements on the electrical driving signals that do not deteriorate the isolation and the level of the generated side bands by more than $1\,\mathrm{dB}$ and find that these requirements can be met using current electronics. The UPM presented here can thus be used in combination with a filter to form an integrated optical isolator.

REFERENCES

[1] B. J. H. Stadler and T. Mizumoto, "Integrated magneto-optical materials and isolators: a review," IEEE Photon. J. **6**, 1–15 (2014).

[2] C. R. Doerr, N. Dupuis, and L. Zhang, "Optical isolator using two tandem phase modulators," Opt. Lett. **36**, 4293–4295 (2011).

[3] T. T. M. van Schaijk, D. Lenstra, E. A. J. M. Bente, and K. A. Williams, "Theoretical analysis of a feedback insensitive semiconductor ring laser using weak intracavity isolation," IEEE J. Sel. Topics Quantum Electron. **24**, no. 1 (2018).

[4] L. M. Augustin *et al.*, "InP-based generic foundry platform for photonic integrated circuits," IEEE J. Sel. Topics Quantum Electron. **24**, no. 1 (2018).